

General Disclaimer

One or more of the Following Statements may affect this Document

- This document has been reproduced from the best copy furnished by the organizational source. It is being released in the interest of making available as much information as possible.
- This document may contain data, which exceeds the sheet parameters. It was furnished in this condition by the organizational source and is the best copy available.
- This document may contain tone-on-tone or color graphs, charts and/or pictures, which have been reproduced in black and white.
- This document is paginated as submitted by the original source.
- Portions of this document are not fully legible due to the historical nature of some of the material. However, it is the best reproduction available from the original submission.

1. REPORT NO. NASA TM X- 64956	2. GOVERNMENT ACCESSION NO.	3. RECIPIENT'S CATALOG NO.	
4. TITLE AND SUBTITLE Monotectic and Syntectic Alloys: ASTP Experiment MA-044 Postflight Preliminary Technical Report		5. REPORT DATE September 30, 1975	
		6. PERFORMING ORGANIZATION CODE	
7. AUTHOR(S) Choh-Yi Ang* and Lewis L. Lacy		8. PERFORMING ORGANIZATION REPORT #	
9. PERFORMING ORGANIZATION NAME AND ADDRESS George C. Marshall Space Flight Center Marshall Space Flight Center, Alabama 35812		10. WORK UNIT, NO.	
		11. CONTRACT OR GRANT NO.	
12. SPONSORING AGENCY NAME AND ADDRESS National Aeronautics and Space Administration Washington, D. C. 20546		13. TYPE OF REPORT & PERIOD COVERED Technical Memorandum	
		14. SPONSORING AGENCY CODE	
15. SUPPLEMENTARY NOTES Prepared by Space Sciences Laboratory, Science and Engineering. Drs. Ang and Lacy are Co-Principal Investigators for ASTP Experiment MA-044. *University Space Research Association.			
16. ABSTRACT <p>The flight test furnace run of Apollo-Soyuz Test Project Experiment MA-044, Monotectic and Syntectic Alloys, was successfully carried out during the Apollo-Soyuz mission. All three experiment cartridges were returned intact. Five of the six samples were successfully extracted from the cartridges. The loss of one aluminum antimonide sample was a result of ampoule failure.</p> <p>Examination of cartridges, ampoules, and external characteristics of samples has been completed. A "quick look" at the microstructures of one aluminum antimonide and one lead-zinc sample was also performed. Pending further in-depth analysis, indications are that a higher degree of compositional homogeneity in aluminum antimonide has been achieved under flight test conditions. Although it is suspected that the lead-zinc samples might not have been soaked at a temperature above the miscibility gap, some interesting microstructure has been observed.</p> <p>A tentative characterization plan has been outlined. The request for a second ground-based test has been made so as to provide one-gravity samples with thermal histories equivalent to those of the flight samples. It is also recommended that a comprehensive thermal analysis be made to determine the actual soaking temperatures during flight testing.</p>			
17. KEY WORDS		18. DISTRIBUTION STATEMENT <i>Lewis Lacy</i> Unclassified - Unlimited	
19. SECURITY CLASSIF. (of this report) Unclassified	20. SECURITY CLASSIF. (of this page) Unclassified	21. NO. OF PAGES 45	22. PRICE NTIS

ACKNOWLEDGMENTS

The authors would like to express their appreciation for the support given to this experiment by Mr. W. R. Adams, Manager of the ASTP MSFC Experiments, and Mr. Arthur Boese, Principal Investigator of the Multipurpose Furnace Experiment MA-010. They would also like to thank the following Marshall Space Flight Center personnel for their efforts and support: Mr. Daniel Gates and Mr. David Nicolas who supplied the SEM/ EDAX data; Mr. James Sandlin who performed the macrophotography; and Mr. Ed Ronning who performed the metallography. The excellent X-radiography was performed by Mr. Paul Duren. The encouragement and advice given to the authors by Dr. Charles Lundquist and Dr. Mathias Siebel are especially appreciated.

TABLE OF CONTENTS

	Page
I. INTRODUCTION	1
II. GENESIS OF EXPERIMENT	1
III. SAMPLE PREPARATION AND PRE-ASTP TESTING	3
A. Thermal Cycling Considerations	3
B. Starting Materials	4
C. Ampoule Configuration and Sample Loading	4
D. Cartridge Construction	4
E. Scheduled Pre-ASTP Tests	5
IV. ASTP FLIGHT TESTING	5
V. PRELIMINARY EVALUATION AND TENTATIVE CHARACTERIZATION PLAN	6
VI. PRELIMINARY EVALUATION RESULTS AND DISCUSSION	7
A. Examination of Cartridges	7
B. Examination of Ampoules	7
C. Preliminary Sample Evaluation	8
VII. INTERIM CONCLUSIONS	10
REFERENCES	37

LIST OF ILLUSTRATIONS

Figure	Title	Page
1.	Phase diagram for PbZn	16
2.	Phase diagram for AlSb	17
3.	Schematic of cartridge and ampoules for ASTP MA-044	18
4.	Exposed view of an instrumented prototype cartridge and ampoules	19
5.	Exposed view of a flight cartridge and ampoules	20
6.	Furnace telemetry data for the heat-up and soak of MA-044	21
7.	Furnace telemetry data for cool-down period of MA-044	22
8.	A comparison of the actual (points on the solid line) and the predicted (dashed curve) thermal profile of MA-044	23
9a.	Low energy X-radiograph of the three flight cartridges	24
9b.	Medium energy X-radiograph of the three flight cartridges	25
9c.	High energy X-radiograph of the three flight cartridges	26
10.	Enlarged X-radiographs of flight AlSb ampoules	27
11.	Enlarged X-radiographs of flight PbZn ampoules	28
12.	Photograph of the flight samples	29
13.	Macrophotograph (5X) of AlSb flight sample 44A164	30
14.	Macrophotograph (10X) of the three PbZn samples	31

LIST OF ILLUSTRATIONS (Concluded)

Figure	Title	Page
15.	Macrograph (10X) of the two ends of PbZn flight sample B181	32
16.	SEM photographs of surface features of PbZn flight sample B181	33
17.	Comparison of the microstructure for a low-gravity and one-gravity solidified AlSb samples (100X)	34
18.	Photomacrograph (8X) of the as-received AlSb starting material	35
19.	Microstructure of PbZn flight sample B186	36

LIST OF TABLES

Table	Title	Page
1.	Thermal History of Available ASTP MA-044 Samples	12
2.	Postflight Evaluation and Characterization Plan for ASTP Experiment MA-044	13
3.	Helium Leak-Test Results of Flight Ampoules	14
4.	Mass of Flight Ampoules Before and After ASTP Flight (g)	14
5.	Mass of Samples in Grams	15

MONOTECTIC AND SYNTECTIC ALLOYS: ASTP EXPERIMENT MA-044

Postflight Preliminary Technical Report

I. INTRODUCTION

This report is primarily a postflight preliminary technical evaluation of the returned samples of aluminum antimonide (AlSb) syntectic compound and lead-zinc (PbZn) monotectic immiscible processed during the Apollo-Soyuz Test Project (ASTP) mission. While the examination of returned cartridges, extracted ampoules, and removed samples was quite detailed in nature, the actual characterization of the space-processed materials has merely begun.

To provide an adequate documentation of the experiment, this report also presents a genesis of the experiment and a summary of efforts and various scheduled tests up to the ASTP mission. From the postflight preliminary examination, a tentative characterization plan has been developed, which makes use of the limited number of available samples and is based on the initial observations. This plan will be modified if new observations at each stage require specialized analytical techniques.

II. GENESIS OF EXPERIMENT

The purpose of ASTP Experiment MA-044, Monotectic and Syntectic Alloys, is to investigate the effects of weightlessness on the melting and solidification of two material systems, namely, PbZn and AlSb. The objectives of the experiment are, therefore, twofold: (1) to investigate phase segregation effects in low gravity for the immiscible binary PbZn and (2) to determine the influences of low-gravity solidification on the microstructural homogeneity and stoichiometry of the semiconducting compound AlSb.

Certain potentially useful alloys or material systems are difficult to synthesize on earth because of large differences in specific gravity of their constituents in the molten state which give rise to undesirable buoyancy and convection influences upon solidification. Consequently, the near-zero gravity condition in space processing was the primary motivation for this experiment. Furthermore, significant discoveries related to microsegregation and kinetics of lattice defects have been made in the Skylab experiments which strengthen the belief in the value of continuing space processing experimentation for future space manufacturing activities.

The PbZn system, as shown by the phase diagram [1] in Figure 1, is characterized by the large miscibility gap ($L_1 + L_2$) and the monotectic point (M) at 99.7 atomic percent Zn, at which the immediate transformation upon solidification is from one liquid to a second liquid plus a solid. This system is also characterized by a large density difference between Pb and Zn (11.7 versus 7.14 g/cm³). In the earth gravity field, it is very difficult to escape from gravity separation between Pb and Zn upon solidification. We hoped that by negating the effects of gravity in space processing, a certain degree of mixing of the two phases could be achieved, resulting possibly in a dispersion of fine particles of superconducting Pb in a Zn matrix. The composition selected for the experiment is 20 atomic percent Pb and 80 atomic percent Zn as shown by the vertical dotted line in Figure 1. This composition is equivalent to 44.2/55.8 Pb/Zn in weight percent, or 33.2/66.8 in volume percent.

Among the III-V semiconducting compounds characterized, upon solidification, by a syntectic transformation of two molten constituents to a constant composition intermetallic compound (50/50 in atomic percent), the aluminum-antimony system (Fig. 2) has been neglected for many years. The reasons for this neglect have been the difficulties [2] in synthesizing a stoichiometrically homogeneous compound and the problems of high reactivity of the material to moisture. Some of the reported properties of AlSb are as follows:

Crystal structure	Zinc-blend
Density	4.27 g/cm ³
Melting point	1050 to 1080°C
Energy gap (20°C)	1.62 eV
Hall mobility (20°C)	
Electrons	200 cm ² /V-s
Holes	420 cm ² /V-s

Dielectric constant	11
Conductivity (p-type)	10^{-2} to $10 \Omega^{-1} \text{ cm}^{-1}$

With an energy gap of 1.62 eV, AlSb has been theoretically analyzed as a highly efficient solar energy converter [3,4]. However, because of the aforementioned problems in crystal synthesis, experimental verification has been conspicuously lacking.

In space processing, we hope that the compositional homogeneity could be enhanced by minimizing the very large density difference ($\text{Al/Sb} = 2.7/6.62$) between constituents in the molten state and during crystallite formation upon cooling. We also suspect, based on electromotive potential considerations, that the Al-rich and Sb-rich phases observed in polycrystalline AlSb synthesized on earth could be the cause for high reactivity to moisture.

III. SAMPLE PREPARATION AND PRE-ASTP TESTING

A. Thermal Cycling Considerations

One AlSb and one PbZn sample were to be processed in each of three flight cartridges. Homogenization (soaking) for 4 hours in the molten state at 850°C for PbZn and at 1100°C for AlSb was originally proposed. The soaking temperature for AlSb was later raised to 1130°C because of the lack of complete melting at 1100°C in laboratory tests and because higher temperatures could not be readily obtained in the Multipurpose Furnace. Unfortunately, despite various reliability measures taken during the processing of laboratory samples and prototype development, the ground-based testing (GBT) encountered serious AlSb sample leakage problems that necessitated a reduction of the soaking time to 1 hour. Including the heat-up and cool-down times for the Multipurpose Furnace, this gave an estimated effective soaking time of 1.8 hours for homogenization of PbZn and 1.6 hours for AlSb.

Temperature and sample-crucible reactivity considerations led to the selection of high-purity POCO brand graphite as the crucible material for both PbZn and AlSb. For the latter, the use of POCO graphite was not an optimum choice, but it was difficult to fabricate alumina crucibles with hermetic sealing for the containment of Al and/or Sb vapor. The reaction between molten AlSb and graphite and the slow carbide formation were recognized and would be taken into consideration in comparing ground and flight samples.

B. Starting Materials

All starting constituents were of material of at least five-nines purity (i. e., total impurities less than 10 ppm). Zinc was in disk form, machined from zone-refined rods. Lead was in both pellet and powder forms. Aluminum-antimonide compound obtained from the Materials Research Corporation was in granular form, processed from zone-refined polycrystalline ingots.

C. Ampoule Configuration and Sample Loading

The ampoule configurations for PbZn and AlSb samples are shown in Figure 3. Briefly stated, the materials were loaded in the graphite crucibles and sealed with graphite cement in an argon glove box. The AlSb samples were premelted at 1150°C in uncapped graphite crucibles under argon before capping and sealing. Tungsten-inert-gas (TIG) welding of the stainless steel ampoule containers was also made in a glove box with approximately 1 atmosphere of ultrahigh purity argon. Both fabricated AlSb and PbZn ampoules were further heated at 1150°C and 850°C for 10 minutes, respectively. For AlSb, the heating was by a high-frequency induction furnace and the thermometry was determined by an optical pyrometer. Lead-zinc ampoules were heated in a 30.5 cm (12 in.) hot zone tube furnace.

Ampoule weighing and ASTM bubble leak testing were performed before and after the heating operation. Graphite boats were used to carry from four to nine ampoules per furnace load. One ampoule of each furnace load was used as a "control" sample. An ampoule might fail the heating test because of either dimensional distortion or leakage. The control samples were further thermally tested for 4 hours at the respective temperatures. If a control failed, the entire boat load was rejected. It should be noted that all PbZn ampoules passed, but one of the five AlSb control ampoules failed. Of the 33 AlSb ampoules processed for prototype, qualification, ground-based, and flight tests and for laboratory studies, a total of six failed, including the control sample just mentioned. Three "good" ampoules were rejected because of the failure of the previously described control sample.

D. Cartridge Construction

The cartridge was designed by Dr. J. McHugh of Westinghouse Research Laboratories. A simplified schematic of the cartridge is shown in Figure 3. Ampoule temperatures were determined during prototype testing by using an

instrumented cartridge shown in Figure 4, which also presents an exposed view of the components of a cartridge, including the A and B ampoules and the graphite, copper, and stainless steel inserts. Figure 5 shows the same exposed components for a flight cartridge.

E. Scheduled Pre-ASTP Tests

Because of the compressed schedule, all required ampoules were fabricated without the benefit of simulation and prototype tests. Therefore, when ground-based testing was finally conducted, the unfortunate occurrence of two failures¹ (AlSb ampoules) out of three cartridges did not leave sufficient time to develop and introduce changes in crucible materials or new ampoule designs. The final decision was made to adopt the previously mentioned shortening of the soaking time from 4 hours to 1 hour for the flight test and to use X-radiography in the selection of flight test cartridges for increased reliability.

As a result of this last minute change, we were actually left with no true one-gravity samples that were thermally treated identically to the flight samples. Table 1 is constructed to depict this situation. The request has been made to have a second ground-based test in order to achieve the primary experiment objective of comparative characterization of samples.

IV. ASTP FLIGHT TESTING

Experiment MA-044 was the last furnace test run during the ASTP mission. The initial heat-up was started at 175:30 Ground Elapsed Time (GET), which corresponds to 2:50 p.m. CDT on July 23, 1975. The run was completed (cartridges extracted) on the morning of July 24, just prior to the jettison of the docking module (and the furnace).

A computer-generated plot of the telemetered furnace temperatures for the graphite heat leveler (hot end) and the heat extractor (cold end) is presented in Figures 6 and 7. The change of slopes seen in the cooling curves of Figure 7 is caused by the injection of helium into the Multipurpose Furnace for the purpose of increasing the cooling rate. Figure 8 compares the time-temperature profile

1. The failure mode was determined to be cracking of the graphite crucibles similar to that which occurred during ampoule fabrication and testing.

of the flight cartridges (points on the solid curve) with a similar profile (dashed curve) predicted from the ground-based test. The actual ground-based test, however, consisted of a 4-hour soak. As can be seen in Figure 8, the flight furnace required an additional 45 minutes to heat up to soak temperature. This additional heat-up time is believed to be caused by a 30°C colder heat extraction temperature (cold end), less efficient thermal shields, and a lower buss voltage on the flight furnace.

The numbers shown in Figure 8 are estimates, based upon equilibrium temperatures obtained in prototype testing, of the temperatures where critical events are occurring inside the cartridges. A more reliable estimate of the critical events must wait until a detailed thermal analysis can be supplied by Marshall Space Flight Center (MSFC). Based upon our initial estimates, the AlSb samples should have been in the homogenization region (i. e., in the liquid state) for 1.6 hours and the PbZn samples in the miscible region (i. e., above the consolute temperature) for 1.8 hours. During the cool-down period, it is estimated that PbZn was in the two-liquid phase region (i. e., the miscibility gap) for 2.9 hours and the liquid Pb-solid Zn region (monotectic region) for 1.1 hours.

The flight cartridge and ampoule numbers are identified as shown in Table 1. Based on the temperature calibration data provided by Westinghouse Research Laboratories and the ground-based test results, the AlSb ampoule temperature at soak is estimated to be 1126°C. Because of the lower cold end temperature, the PbZn ampoule temperature at soak was estimated to be below 850°C. As discussed in a later section, there is evidence that the PbZn might not have been homogenized in a miscible temperature region.

V. PRELIMINARY EVALUATION AND TENTATIVE CHARACTERIZATION PLAN

Without going into details, the tentative postflight evaluation and characterization plan for the returned samples is shown in Table 2.

This report covers efforts performed under tasks 1 and 2 and through subtask (f) of task 3. Additionally, a "quick look" at the microstructures of the one AlSb sample and one PbZn sample has also been included.

VI. PRELIMINARY EVALUATION RESULTS AND DISCUSSION

A. Examination of Cartridges

All three cartridges were in excellent condition and showed no evidence of leakage. Figure 9 shows positive images of the X-radiographs for the three cartridges using different X-ray energies. Figure 9a corresponds to the least penetrating X-rays, where the relative location of the A ampoules and the copper thermal insert containing the B ampoules can be seen. Figure 9b shows a more penetrating view of the cartridges where the three AlSb samples inside of the A ampoules can be seen. Small cracks are evident in the graphite crucible of cartridge 7, and the ampoule in cartridge 9 (center cartridge) shows evidence of cracks and leakage of AlSb around the ampoule (i.e., gray region of the ampoule). The A ampoule in cartridge 10 shows no evidence of cracking. Thus, the ampoules in cartridges 7 and 10 appear to be in good shape. The more penetrating view of Figure 9c shows the three B ampoules containing the PbZn samples. The three B ampoules were in excellent condition. Comparing Figures 9a and 9b, it was concluded that none of the leaking AlSb in cartridge 9 escaped from the graphite thermal insert of the cartridge.

B. Examination of Ampoules

After removal of the ampoules from the cartridges, X-radiographs of the ampoules were taken. Enlarged (magnification 4X) positive images of the ampoules can be seen in Figures 10 and 11. As shown in Figure 10, a major crack developed in ampoule 44A184 (cartridge 9). Since the X-radiographs of the AlSb ampoules were taken under the same exposure conditions, the relatively dark areas of 44A184 show evidence of AlSb leakage. No evidence of leakage appears for the other two ampoules (44A185 and 44A167). In Figure 11, the enlarged (4X) images of the X-radiographs show definite structure in the PbZn samples. Since Pb has ten times more absorptivity for X-rays than does Zn, ampoules B181 and B164 appear to have wider zones of mixed components than ampoule B185. Later cross-sectioning of the sample will determine the actual distribution of the two components.

After X-radiographs were taken, each ampoule except 44A187 was helium leak-tested. The leak-test results are presented in Table 3. The leak test indicated no significant leaks in any of the ampoules.

The mass of each ampoule was determined before and after flight, and the results are presented in Table 4. There was no significant mass change for any ampoules except 44B181 and 44A184. The mass increase (339.7 mg) associated with 44A184 was caused by an interaction of the leaking AlSb with the graphite insert that was partially stuck to the ampoule. The mass decrease of 44B181 (42.4 mg) was caused by a small loss of stainless steel from the ampoule while machining away part of the copper insert.

Combining the results of X-radiography, helium leak-testing, and mass determination, it was concluded that there were two good AlSb and three good PbZn samples which would be investigated as specified by task 3.

C. Preliminary Sample Evaluation

The stainless steel jackets of the ampoules were carefully cut open on a lathe. With the PbZn ampoules, the graphite crucibles were easily pushed out of the opened stainless steel jackets. The PbZn samples slipped out of the crucibles easily. The graphite crucibles for both AlSb samples could not be pushed out of the stainless steel ampoules, and a jeweler's saw was used to cut open the ampoules. The AlSb samples were stuck to the crucibles as anticipated. Splitting open the graphite crucibles resulted in one stripped A164 AlSb ingot consisting of about 89 percent of the original mass, and one-half ampoule containing the A185 AlSb sample.

From available data, Table 5 is constructed showing preflight and post-flight weights of the samples. Because of the anticipated reaction between AlSb and graphite, no accurate post-ASTP mass determination can be made. With the PbZn samples, on the other hand, we are quite confident about the results of mass determination. The weight losses of 1.5 and 0.8 percent for B181 and B164 are not unexpected because of the vaporization and condensation on machined crevices of the graphite walls and screw threads. The 7.15 percent weight loss of B186 appears to be somewhat excessive and its cause cannot be determined at this time.

Figure 12 is a photograph of the two AlSb and three PbZn samples. Part of the graphite crucible was left attached to A185 so that later microstructure analysis could be correlated with potential contamination by the graphite crucible. Visual observation of the exposed surfaces of the AlSb samples indicated that melting and recrystallization did occur. A macrophotograph (5X) of one of the AlSb samples (44A164) can be seen in Figure 13 where large crystallites of the polycrystalline sample can be seen. Part of the graphite crucible can also be seen on the bottom of the sample.

Complete melting had also occurred with the three PbZn samples. Macrophotography (10X) of the samples can be seen in Figure 14. As shown in Figure 14, an interface exists between a smaller and larger part of the samples. This interface may correspond to the original Pb/Zn interface. Overflow regions can be seen on the surface of the sample where a liquid phase flowed over the first solidified surfaces.

Each of the samples appears to have solidified first on the cold end (temperature gradient of $4.5^{\circ}\text{C}/\text{cm}$), and because of shrinkage away from the container walls, part of the remaining liquid then flowed around the solid surface. The topography of sample B186 appears to be different from the other two samples. In sample B186, the liquid flow appears to be symmetric about the axis of the sample, whereas on sample B164 an asymmetric flow channel apparently developed. Sample B181 also has an asymmetric flow, as can be seen in Figure 15 which is a photograph of its cold end.

A closer examination of B181 in Figure 14 reveals small parallel grooves or strata around the circumference of the sample. These grooves are believed to be caused by machining marks in the graphite crucible. A more detailed view of the topography of B181 is shown in the SEM photographs of Figure 16. A shrinkage cavity is visible on the hot end of the sample (Fig. 16a), and the interface region is shown in Figure 16b. A preliminary EDAX of B181 reveals that both Pb and Zn are present at both the hot and cold ends of the sample and that the concentration of Zn is more pronounced at the cold end.

For a preliminary microstructural examination, we decided to mount and cut one longitudinal section each of the A185 AlSb sample and B186 PbZn sample for metallography. It should be emphasized here that the examination was intended to provide only a "quick look" on the gross microstructural features which may form a basis for subsequent detailed characterization procedures for in-depth analysis.

The flight AlSb sample appears to have an overall homogeneous phase with a small amount of a second phase along the grain boundaries. Figure 17a illustrates this typical feature (unetched). With all the AlSb samples processed on the ground, including the as-received AlSb granule, one sees at least two phases — one rich in Sb, and the other the compound AlSb. Figure 17b shows this feature of large amounts of two phases present in one-gravity solidified samples. The one-gravity solidified sample (A127) was obtained in a prototype test that had approximately the same thermal history as the ASTP solidified sample. A more

detailed comparison will be made as soon as ground-based samples with the same thermal history as the flight samples are processed. Figure 18 is a macrophotograph at 8X of one of the large AlSb granules, as received from the supplier, which also exhibits the duplex microstructural features.

While much work had been done on earlier laboratory samples in identifying qualitatively the Al and Sb concentration of the grey and white phases, it is our intention to perform energy dispersive X-ray analysis on the flight samples and ground-based test samples prior to presenting a detailed discussion. The preliminary observations thus far do indicate a higher degree of compositional homogenization in the flight sample as compared to polycrystalline counterparts processed on earth.

The flight sample of PbZn (B186) exhibits a microstructure not unlike that of ground samples, i. e., a zinc portion and a lead portion (intrapping one large and several small zinc particles, see Fig. 19a). At this time, it is difficult to visualize the incomplete interdiffusion between Pb and Zn atoms in the molten state, unless the sample failed to reach a temperature beyond the miscibility gap [5, 6].

From Figure 19b, one sees some striking features (5 percent HNO₃ etched) of crystallite formation in zinc. There are also small particulate inclusions or etched pits, as shown in Figures 19b and 19c. A preliminary EDAX scan indicated that the zinc matrix contains lead. One cannot rule out, however, the possibility of lead smearing during the final stages of etching and polishing. A ground sample with a similar history must be analyzed by EDAX to clear up this point. Other material removal techniques, such as ion-etching, may have to be used to avoid surface contamination in inclusion identification.

VII. INTERIM CONCLUSIONS

Except for the factual observations made in examining the cartridges and ampoules, the "quick look" metallography must be considered as very much tentative in nature. With this in mind, one can present the following remarks:

1. Five out of six samples have been successfully recovered from the flight test.
2. The flight test appeared to have followed the programmed thermal cycle except for the colder end temperature, which makes it difficult to estimate the soak temperature of the PbZn ampoules.

3. All recovered samples appear to be in good condition. One PbZn ingot has a somewhat high weight loss of 7.9 percent. Both the AlSb and PbZn show definite evidence of melting and resolidification in low gravity.

4. A preliminary microstructure examination of AlSb shows definite improvement in the homogeneity of the ASTP solidified material in comparison with one-gravity solidified samples. A small amount of a second phase was found only at the grain boundaries in the low-gravity solidified material. This observation of a high degree of homogenization in one flight AlSb sample must be verified further by a more extensive analysis during formal characterization.

5. Incomplete homogenization between Pb and Zn has been observed in one flight sample. This is believed to be caused by the soak temperature being below the consolute temperature of the binary system. Although complete homogenization was not achieved in the PbZn system, the presence of fine Pb particles was detected in the Zn matrix by a preliminary EDAX study.

6. Flow patterns, where a liquid phase flows over the first solidified phases, have been observed in the PbZn samples. Such fluid motion in zero gravity could affect the microstructure of the resulting alloy.

7. A second ground-based testing should be made to provide equivalent one-gravity samples for comparative characterization.

8. A thermal analysis must be made to determine the true soaking temperatures of the two zones and to determine the furnace temperatures corresponding to critical events (i.e., melting points and consolute temperature) of the samples.

TABLE 1. THERMAL HISTORY OF AVAILABLE ASTP MA-044 SAMPLES

Test Origin	Cartridge No.	Ampoule/Sample	Thermal History ^a
Flight	7	A185/AlSb	1° @ 1126°C
Flight	10	A164/AlSb	1° @ 1126°C
Flight	7	B186/PbZn	1° @ ~ 850°C
Flight	9	B181/PbZn	1° @ ~ 850°C
Flight	10	B164/PbZn	1° @ ~ 850°C
GBT	1	A163/AlSb	4° @ 1132°C
GBT	1	B160/PbZn	4° @ 865°C
GBT	2	B161/PbZn	4° @ 865°C
GBT	3	B162/PbZn	4° @ 865°C
Proto-2	1	A124/AlSb	5.6° @ 1049°C + 1.3° @ 1132°C
Proto-2	2	A132/AlSb	1.2° @ 1112°C + 1.3° @ 1132°C
Proto-2	3	A126/AlSb	1.2° @ 1112°C + 1.3° @ 1132°C
Proto-2	1	B124/PbZn	5.6° @ 741°C + 1.3° @ 865°C
Proto-2	2	B125/PbZn	1.2° @ 935°C + 1.3° @ 865°C
Proto-2	3	B105/PbZn	1.2° @ 935°C + 1.3° @ 865°C

a. 1 @ 1126°C denotes a 1-hour soak time at 1126°C.

TABLE 2. POSTFLIGHT EVALUATION AND CHARACTERIZATION
PLAN FOR ASTP EXPERIMENT MA-044

	AlSb	PbZn
Task 1: <u>Cartridge Examination</u>		
(a) Photography	X	X
(b) Radiography (Before and After Flight)	X	X
(c) Disassembly	X	X
Task 2: <u>Ampoule Examination</u>		
(a) Photography	X	X
(b) Radiography	X	X
(c) Leak Tests (Helium)	X	X
(d) Weighing	X	X
Task 3: <u>Sample Characterization</u>		
(a) Removal	X	X
(b) Weighing	X	X
(c) Stereoscopic Examination (10X to 100X)	X	X
(d) Macrophotography (2X to 10X)	X	X
(e) SEM Topography (60X to 1000X)	No	X
(f) Surface EDAX	No	X
(g) Microstructure (Metallography)	X	X
(h) Microhardness Testing	X	?
(i) SEM/ EDAX (Qualitative and Quantitative)	X	X
(j) Resistivity (4-Point Probe)	X	X
(k) Superconductivity	No	X
(l) X-Ray Diffraction	X	X
(m) Chemical and Spectral Analysis	X	X
(n) Impurity Analysis (Ion Microprobe)	X	?
(o) Spreading Resistance	?	No
(p) Humidity Oven Testing	X	No

TABLE 3. HELIUM LEAK-TEST RESULTS
OF FLIGHT AMPOULES

Ampoule Number	Leak Rate (st cm ³ /s)	Leak Status
44B181	6×10^{-10}	OK
44B164	4×10^{-10}	OK
44B186	2×10^{-10}	OK
44A185	6×10^{-7}	OK
44A164	2×10^{-9}	OK
44A184	-	Leaked

TABLE 4. MASS OF FLIGHT AMPOULES BEFORE
AND AFTER ASTP FLIGHT (g)

Cartridge Number	Ampoule Number	Pre-ASTP	Post-ASTP	Weight Change	Percent Change
07	44B186	6.7190	6.7118	-0.0072	-0.11
07	44A185	12.5135	12.5160	-0.0025	-0.02
09	44B181	6.8960	6.8536	-0.0424	-0.62
09	44A184	12.6321	12.9718	+0.3397	+2.7
10	44B164	6.7679	6.7612	-0.0067	-0.10
10	44A164	12.7524	12.7500	-0.0024	-0.02

TABLE 5. MASS OF SAMPLES IN GRAMS

Sample	Prc-ASTP	Post-ASTP	Weight Loss	Percent Loss
B186 PbZn	1.3009	1.2077	0.0932	7.15
B181 PbZn	1.3263	1.3065	0.0198	1.50
B164 PbZn	1.3609	1.3500	0.0109	0.80
A185 AlSb	2.7231	2.4123 ^a	-	-
A164 AlSb	2.6221	-	-	-

a. 11 percent of mass is adhered to graphite crucible wall due to reaction.

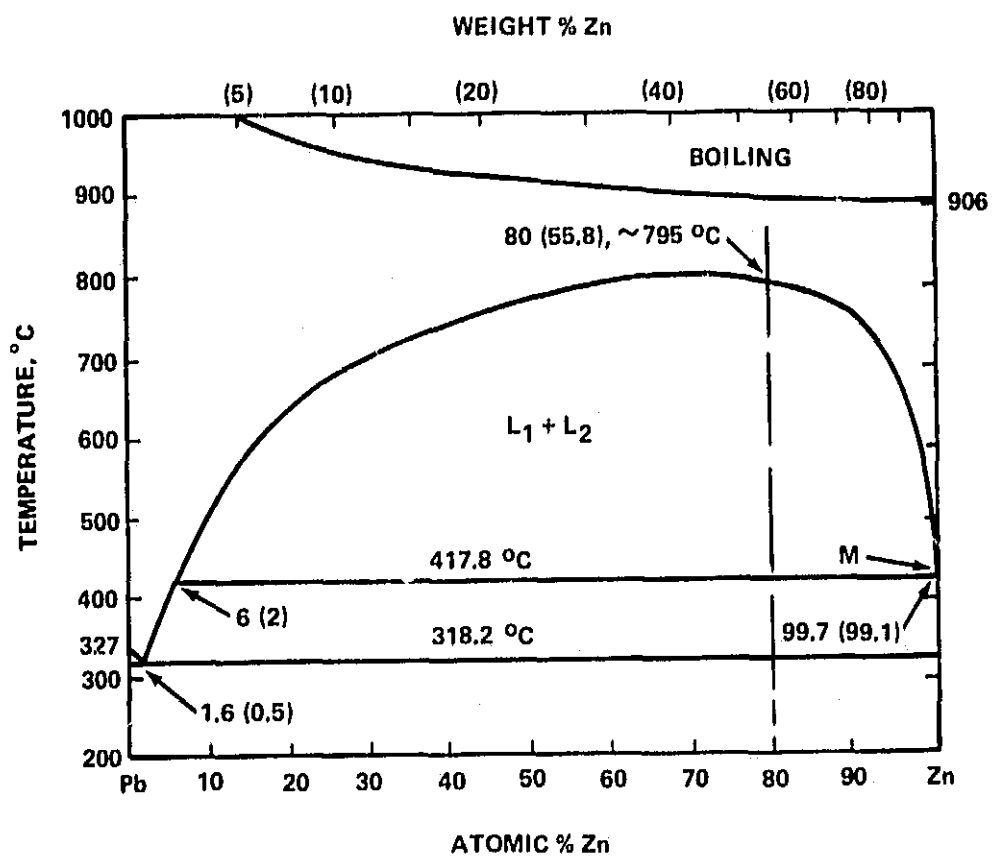


Figure 1. Phase diagram for PbZn.

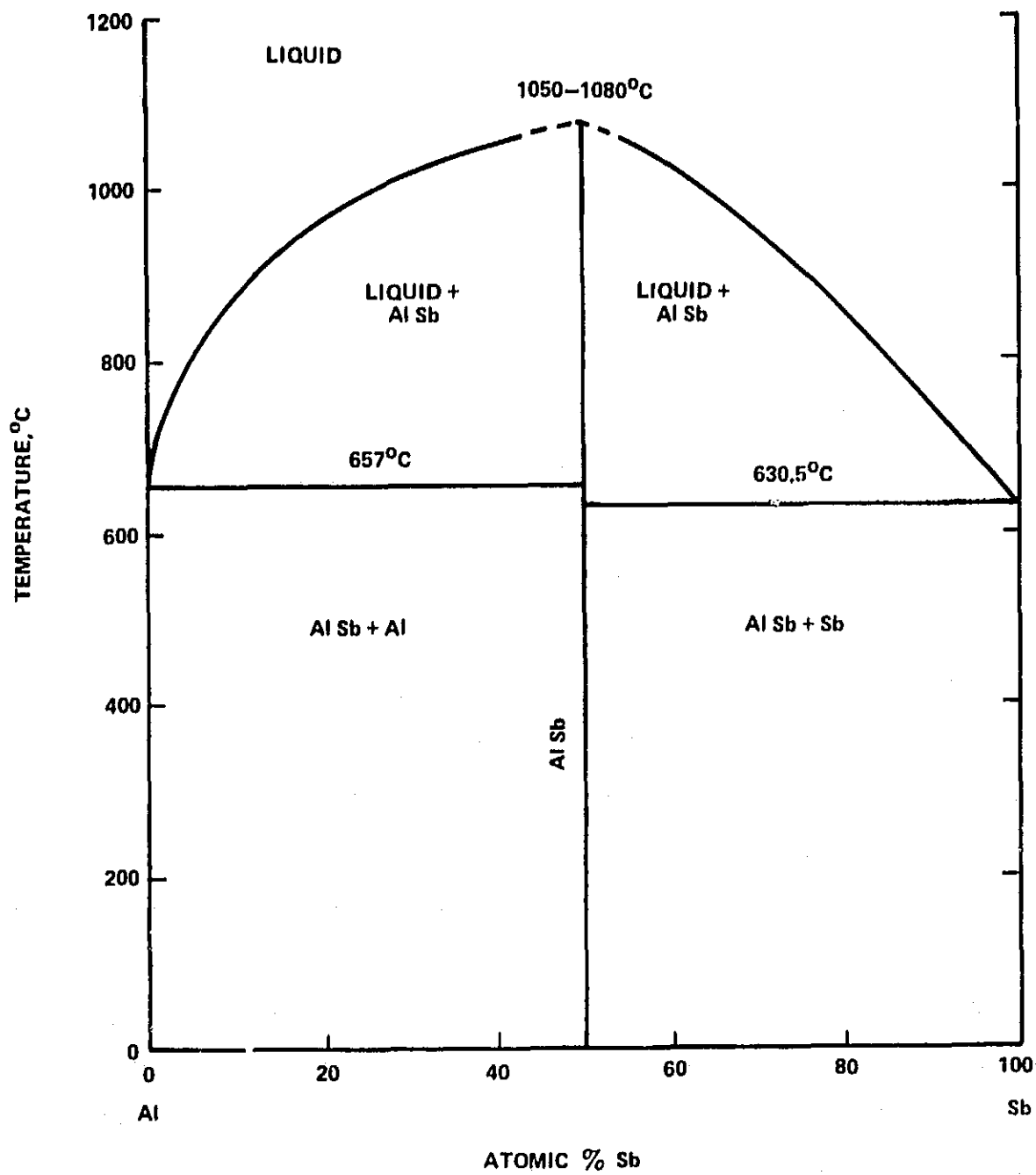
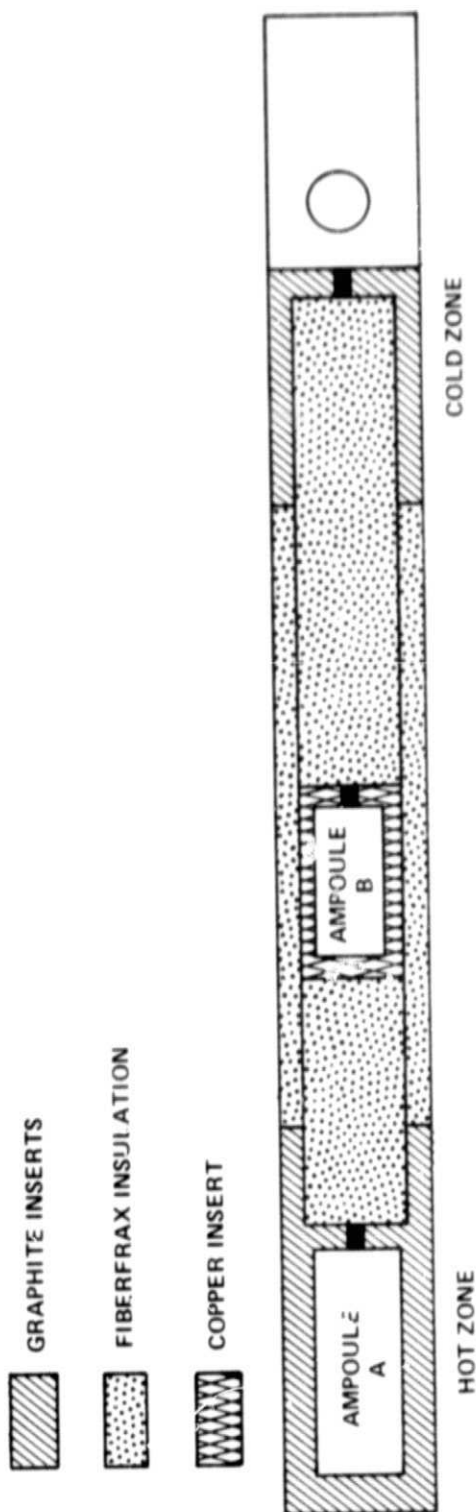
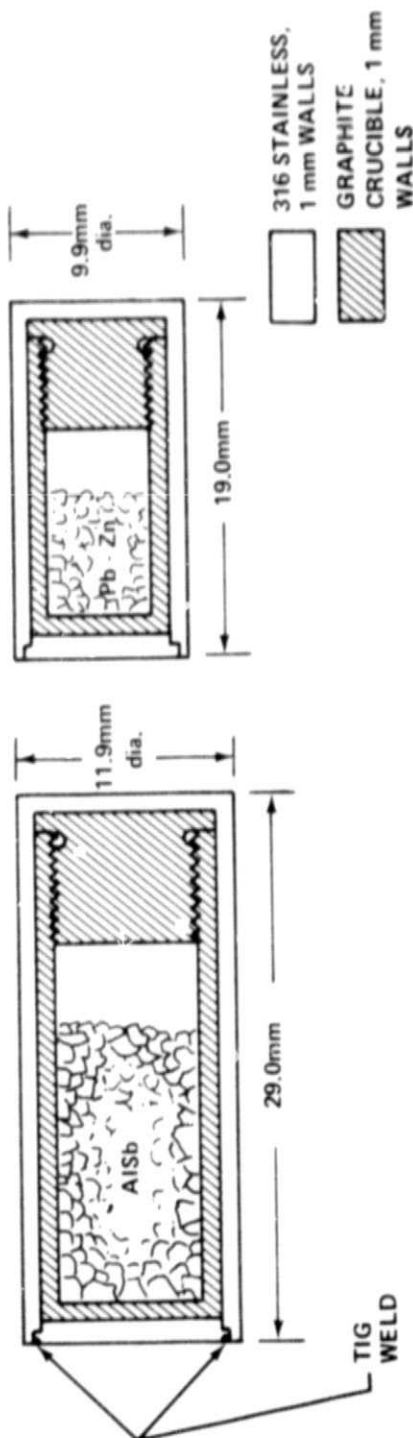


Figure 2. Phase diagram for AlSb.



a. Simplified schematic of stainless steel cartridge assembly.



c. Ampoule B (PbZn).

b. Ampoule A (AlSb).

Figure 3. Schematic of cartridge and ampoules for ASTP MA-044.

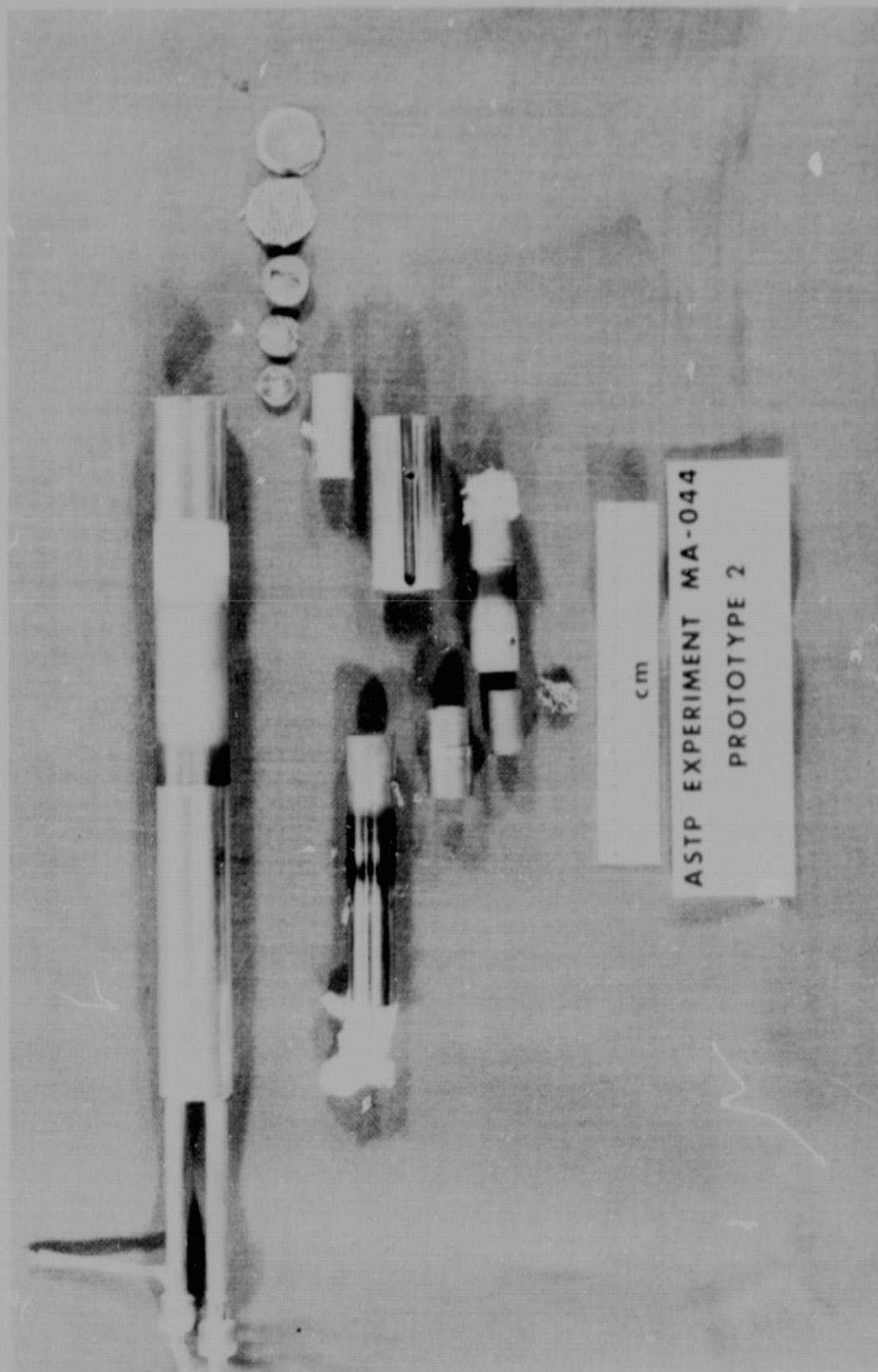


Figure 4. Exposed view of an instrumented prototype cartridge and ampoules.

ORIGINAL PAGE IS
OF POOR QUALITY

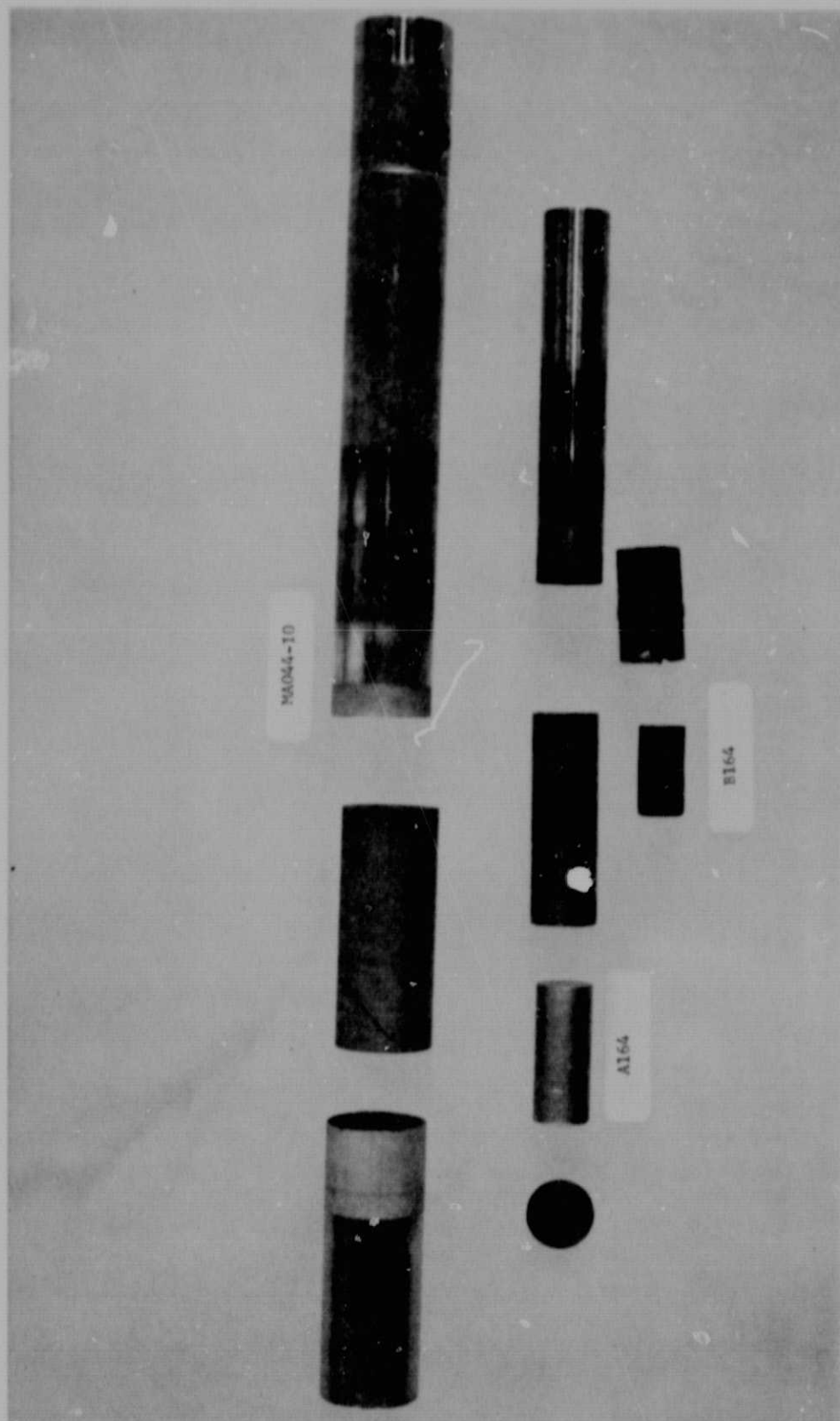


Figure 5. Exposed view of a flight cartridge and ampoules.

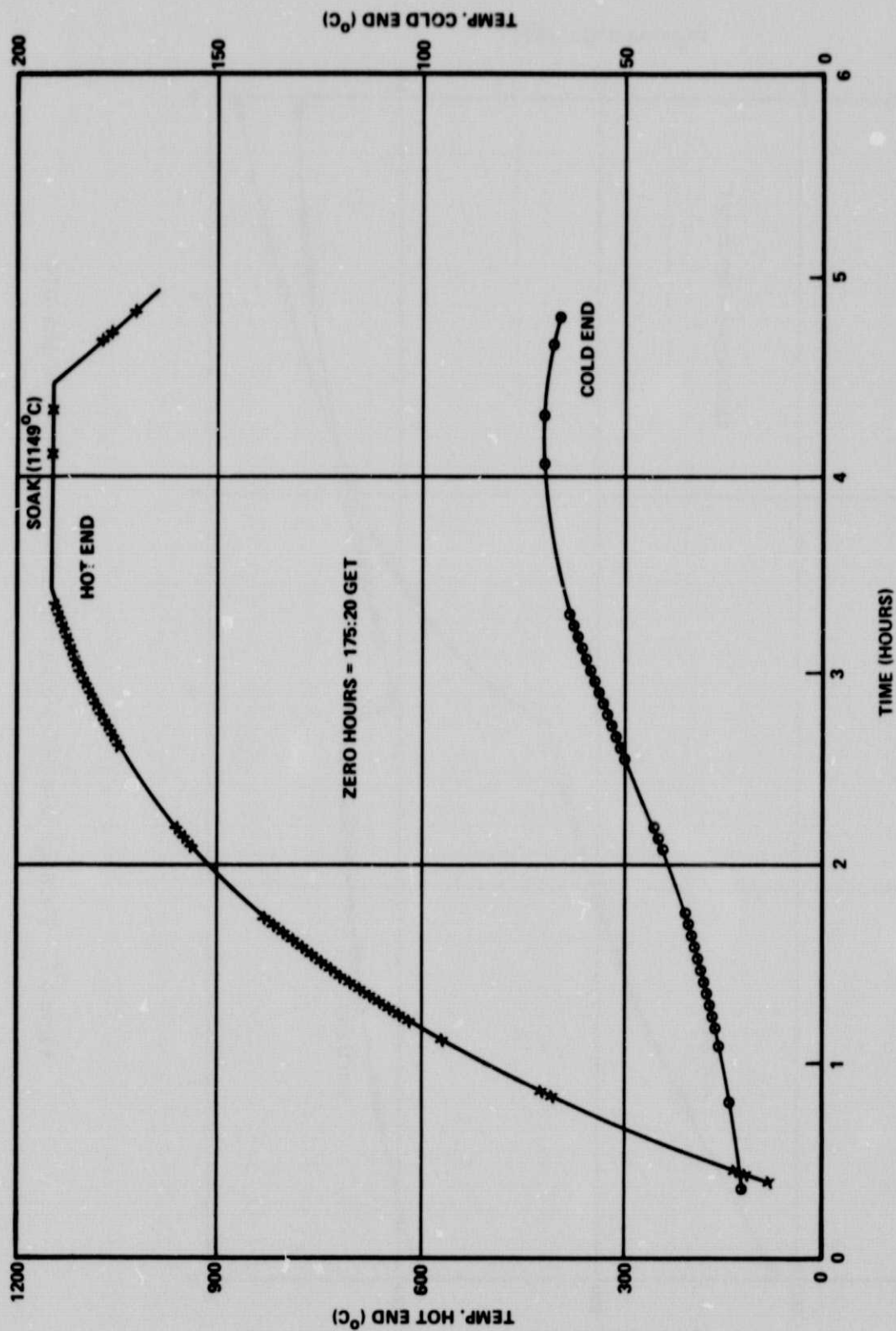


Figure 6. Furnace telemetry data for the heat-up and soak of MA-044.

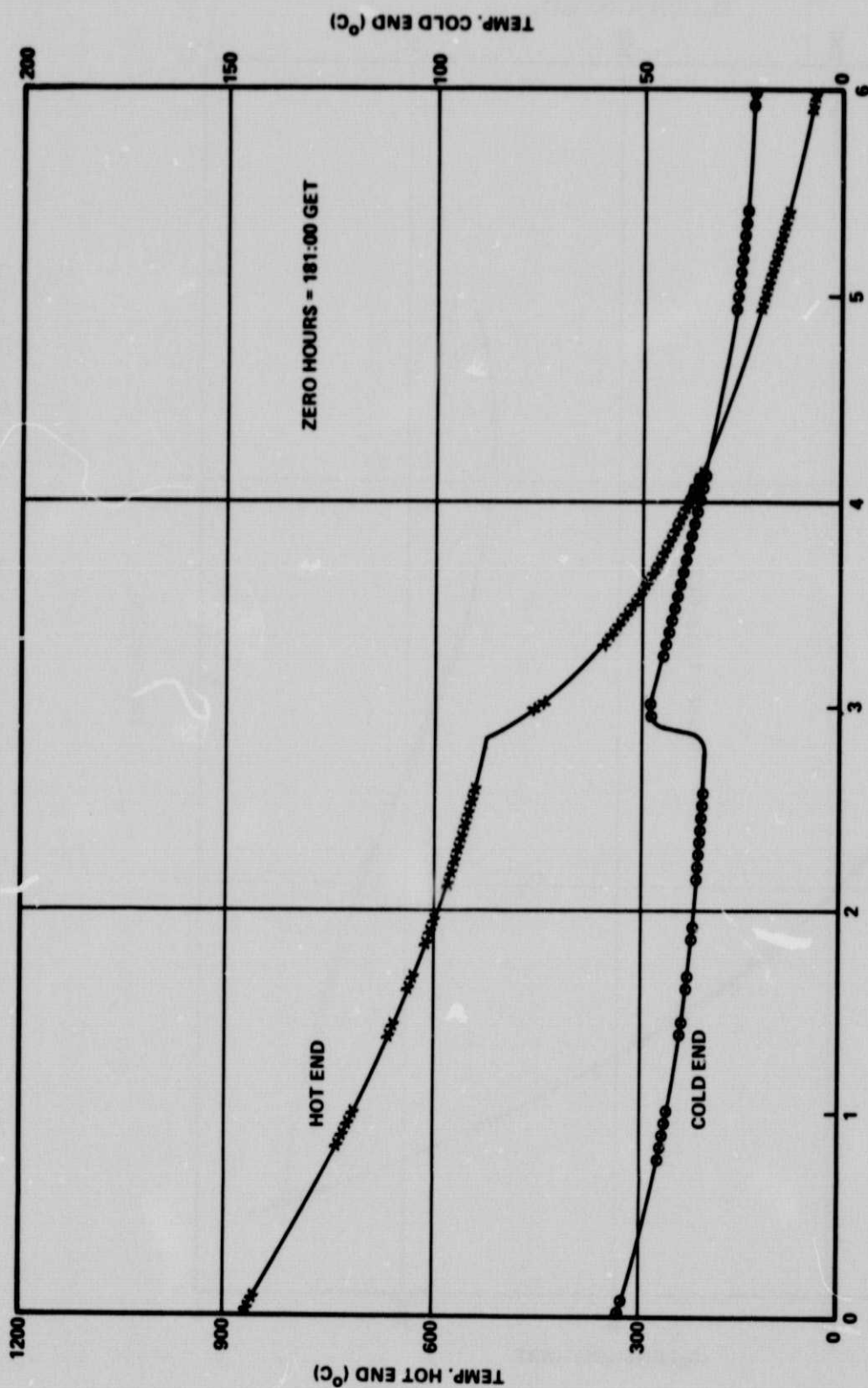


Figure 7. Furnace telemetry data for cool-down period of MA-044.

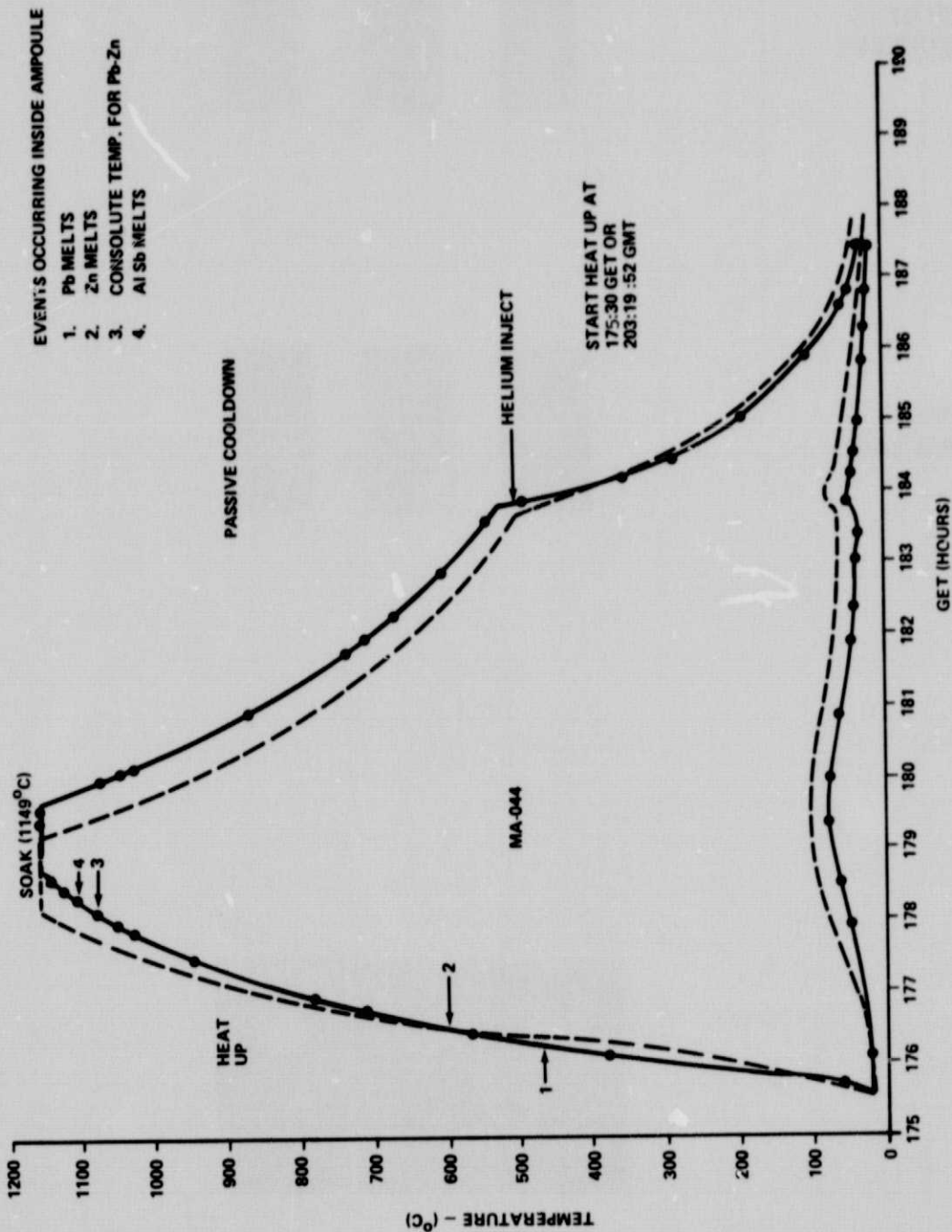


Figure 8. A comparison of the actual (points on the solid line) and the predicted (dashed curve) thermal profile of MA-044.

CARTRIDGE NO.

7

9

10

LOCATION OF
Al Sb AMPOULES

LOCATION OF
Pb Zn AMPOULES

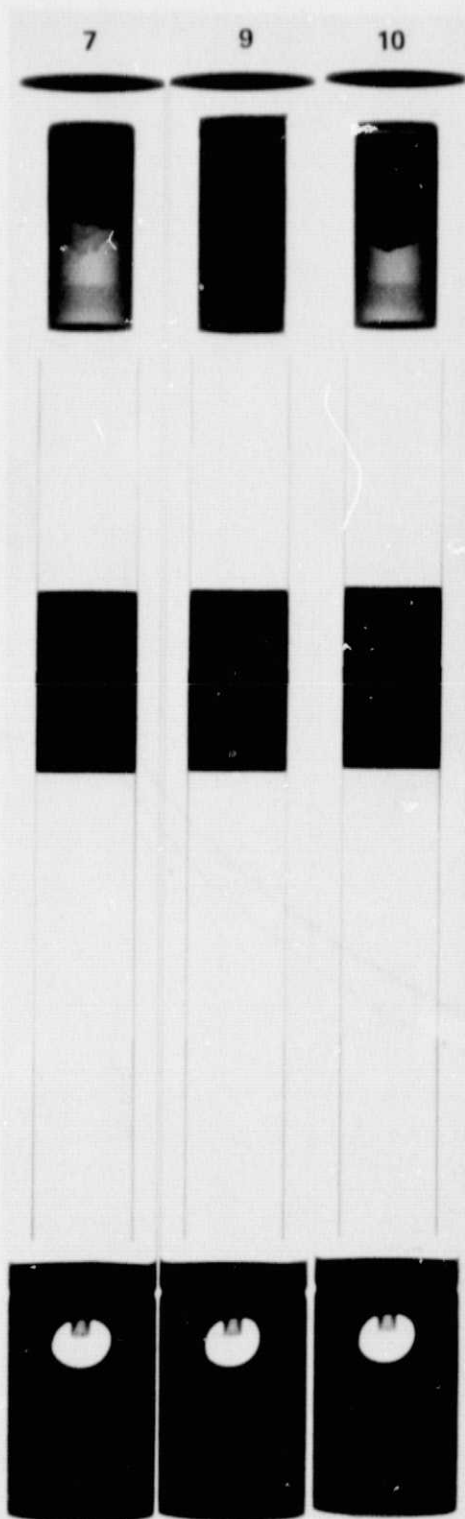


Figure 9a. Low energy X-radiograph of the three flight cartridges.

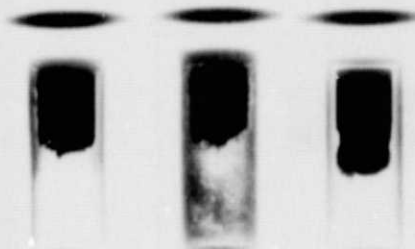
CARTRIDGE NO.

7

9

10

LOCATION OF
Al Sb AMPOULES



LOCATION OF
Pb Zn AMPOULES



Figure 9b. Medium energy X-radiograph of the three flight cartridges.

CARTRIDGE NO.

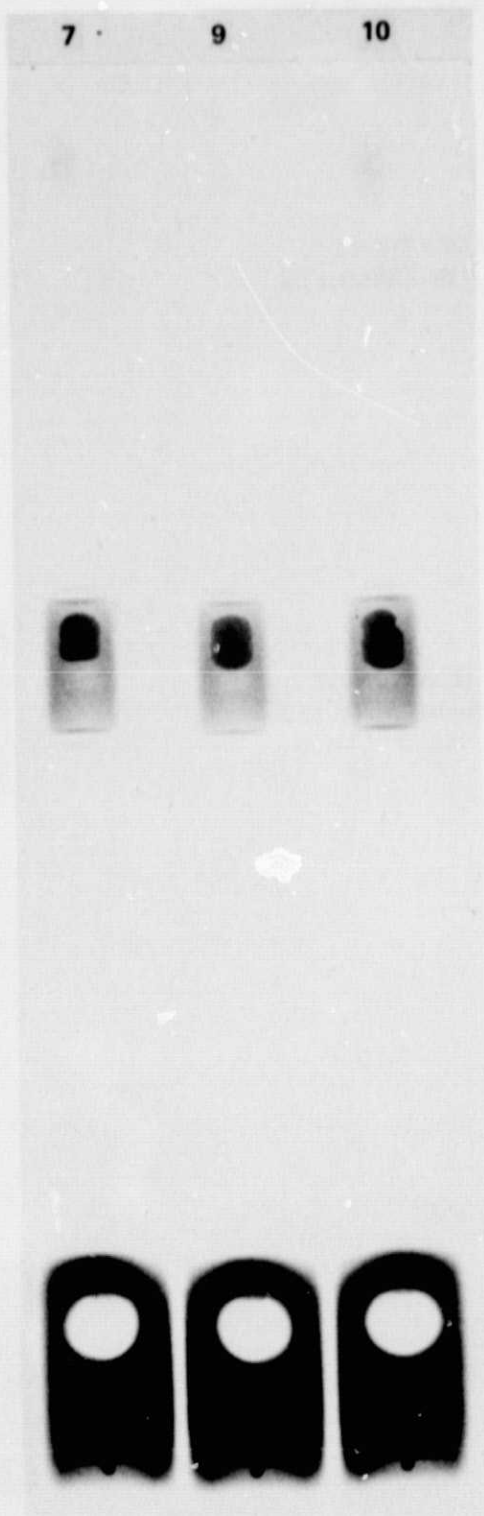
7

9

10

**LOCATION OF
Al Sb AMPOULES**

**LOCATION OF
Pb Zn AMPOULES**



**ORIGINAL PAGE IS
OF POOR QUALITY**

Figure 9c. High energy X-radiograph of the three flight cartridges.

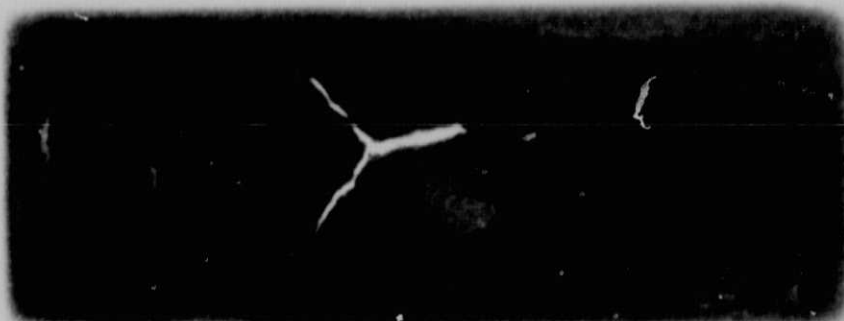
CARTRIDGE: MA-044-07
AMPOULE: 44A185

MA-044-09
44A184

MA-044-10
44A164



HOT END



HOT END

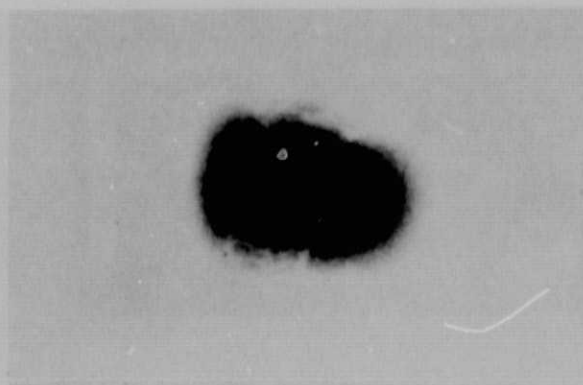


HOT END

ORIGINAL PAGE IS
OF POOR QUALITY

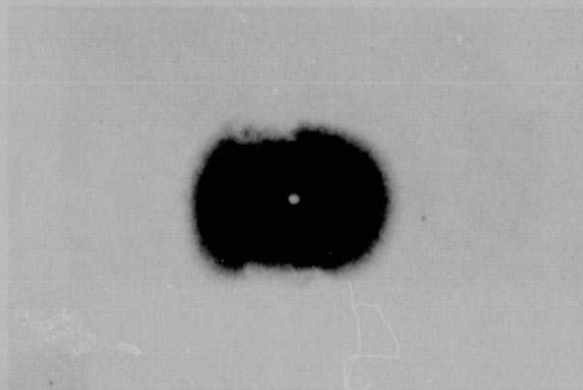
Figure 10. Enlarged X-radiographs of flight AlSb ampoules.

MA-044-10
44B164



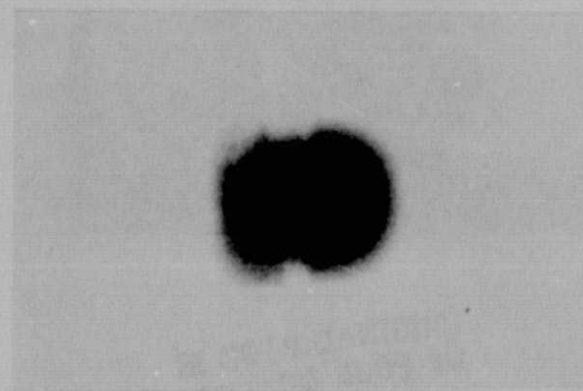
HOT END

MA-044-09
44B181



HOT END

CARTRIDGE: MA-044-07
AMPOULE: 44B186



HOT END

Figure 11. Enlarged X-radiographs of flight PbZn ampoules.

ASTP EXPERIMENT MA 044

A 185



B 186



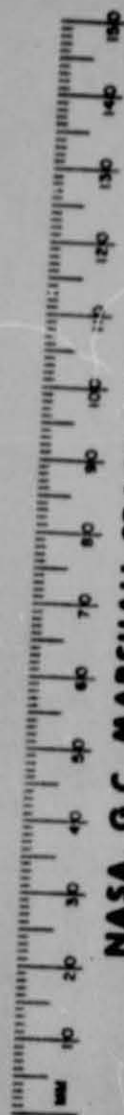
A 164



B 181



B 164



NASA, G.C. MARSHALL SPACE FLIGHT CENTER

SPACE SCIENCES LABORATORY

Figure 12. Photograph of the flight samples.

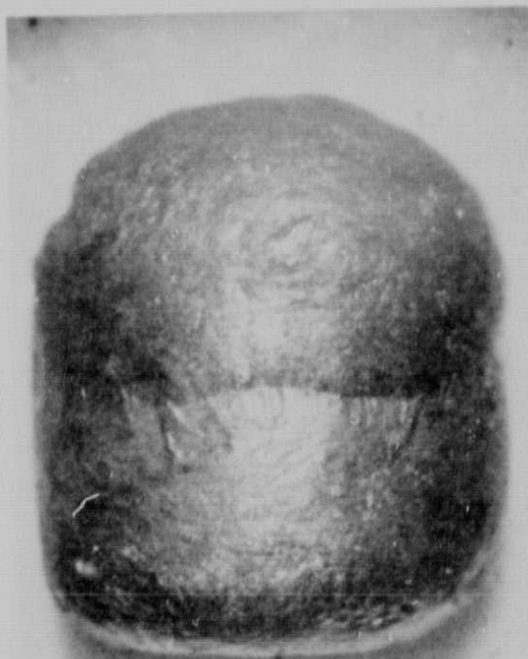


Figure 13. Macrophotograph (5X) of AlSb flight sample 44A164.

B181



B186



HOT
END →

5mm

B164

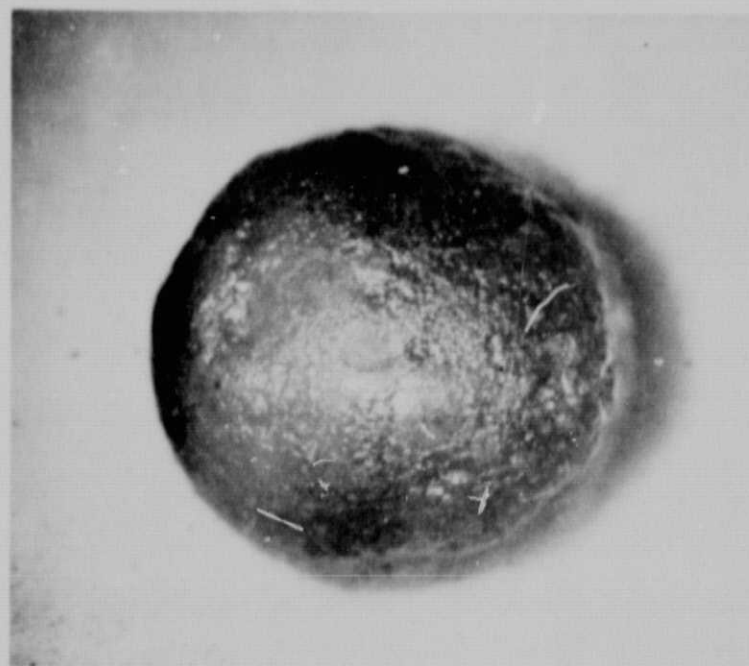


ORIGINAL PAGE IS
OF POOR QUALITY

Figure 14. Macro photograph (10X) of the three PbZn samples.



COLD END



HOT END

5mm

Figure 15. Macro photograph (10X) of the two ends of PbZn flight sample B181.

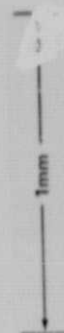
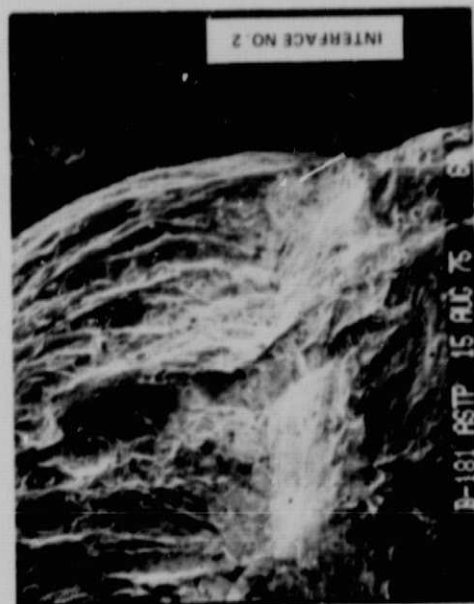
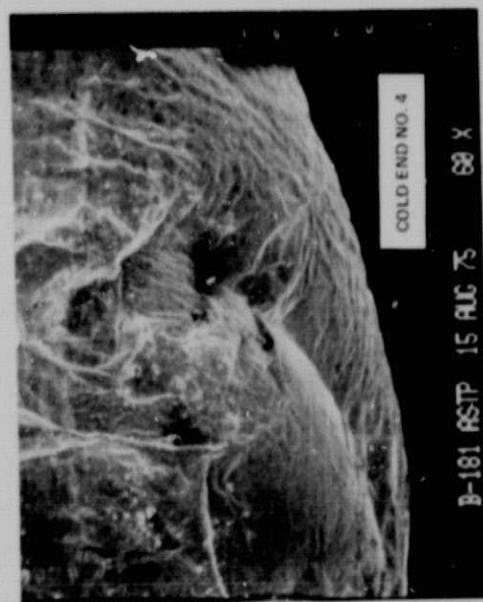
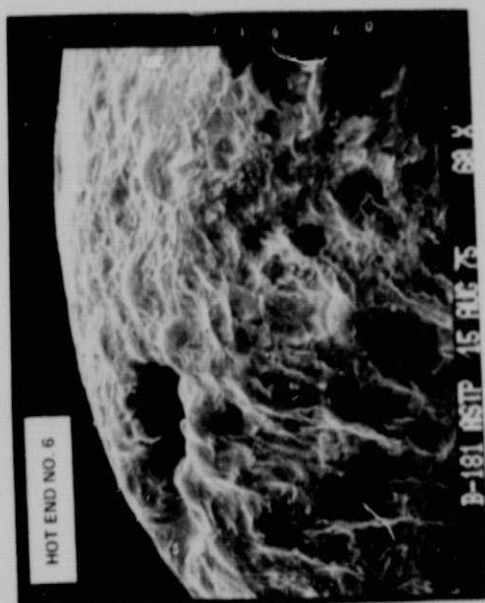
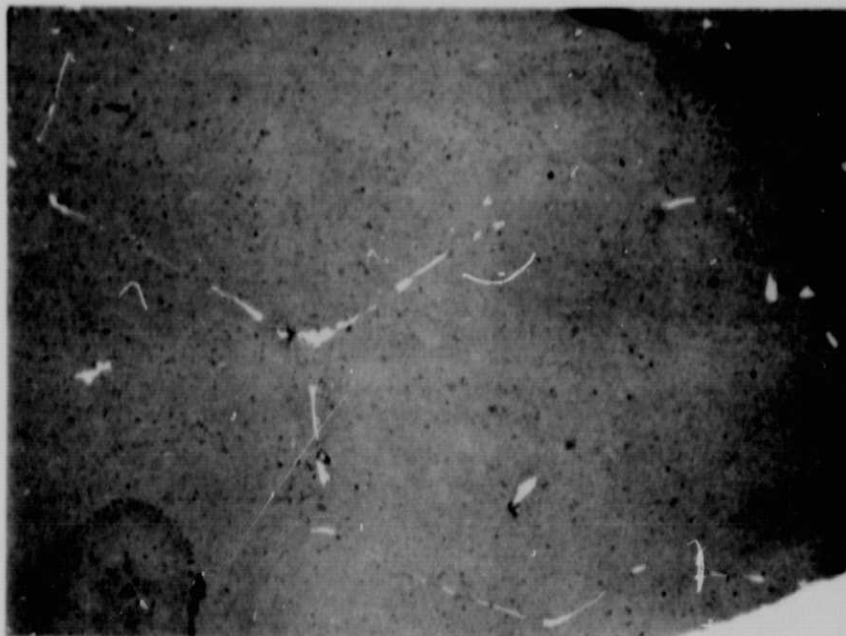


Figure 16. SEM photographs of surface features of PbZn flight sample B181.

a



LOW g
(A185)

b



ONE g
(A127)

Figure 17. Comparison of the microstructure for a low-gravity and one-gravity solidified AlSb samples (100X).

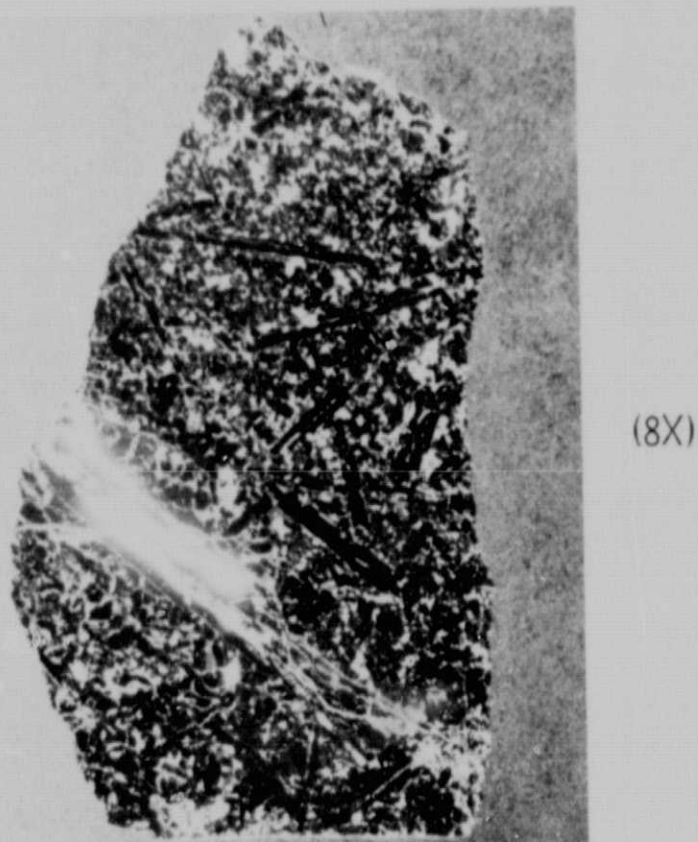
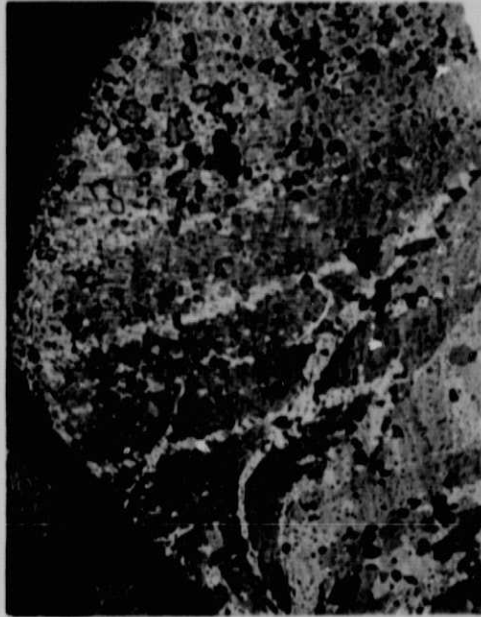


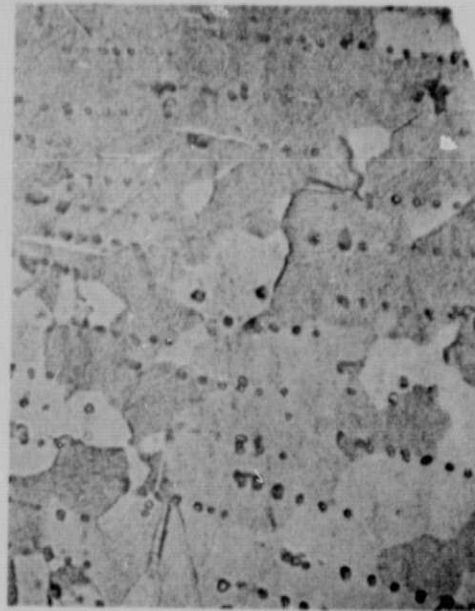
Figure 18. Photomicrograph (8X) of the as-received AlSb starting material.



a. 10X



b. 50X



c. 500X

Figure 19. Microstructure of PbZn flight sample B186. (Note: Figure was reduced for printing.)

REFERENCES

1. Modified from Hansen, M.: Constitution of Binary Alloys. McGraw-Hill, New York, 1958, p. 1118.
2. Willardson, R. K. and Beer, Albert C., eds.: Semiconductors and Semimetals. Vol. 4, Academic Press, New York, 1968, p. 59.
3. Rittner, E. S.: Use of p-n Junctions for Solar Energy Conversion. Physical Review, vol. 96, 1954, p. 1708.
4. Loferski, J. J.: Theoretical Considerations Governing the Choice of the Optimum Semiconductor for Photovoltaic Solar Energy Conversion. J. Applied Physics, vol. 27, 1956, pp. 777-784.
5. Rosenthal, F. D.; Mills, G. J.; and Dunkerley, F. J.: Thermodynamic Study of Liquid Pb-Zn Solutions. Transactions of Metallurgical Soc. of AIME, April 1958, pp. 153-161.
6. Cafasso, F. A.; Feder, Harold M.; and Johnson, Irving: Partition of Solutes between Liquid Metals II, The Lead-Zinc System. J. of Physical Chemistry, vol. 68, 1964, pp. 1944-1948.

APPROVAL

MONOTECTIC AND SYNTECTIC ALLOYS: ASTP EXPERIMENT MA-044

Postflight Preliminary Technical Report

By Choh-Yi Ang and Lewis L. Lacy

The information in this report has been reviewed for security classification. Review of any information concerning Department of Defense or Atomic Energy Commission programs has been made by the MSFC Security Classification Officer. This report, in its entirety, has been determined to be unclassified.

This document has also been reviewed and approved for technical accuracy.



EUGENE W. URBAN

Chief, Low Temperature and Gravitational Sciences Branch



For RUDOLF DECHER

Chief, Radiation and Low Temperature Sciences Division



CHARLES A. LUNDQUIST

Director, Space Sciences Laboratory